

# ANOMALOUS INTERACTIONS IN HIGGS BOSON PRODUCTION AT PHOTON COLLIDERS

A.T. Banin, I.F. Ginzburg\*, I.P. Ivanov  
Institute of Mathematics, Novosibirsk, Russia

## Abstract

We discuss the potentialities of the non-standard interaction study via the Higgs boson production at photon ( $\gamma\gamma$  and  $e\gamma$ ) colliders. We estimate what scale of New Physics phenomena beyond  $\mathcal{SM}$  can be seen in the experiments with Higgs boson production. In particular, the effect of new heavy particles within  $\mathcal{SM}$  is shown to be well observable.

## 1 Introduction

The Higgs boson ( $H$ ) discovery is the key problem of the modern particle physics. A crucial point for the Standard Model ( $\mathcal{SM}$ ), the Higgs boson still remains elusive in the experiments being conducted now. It is expected that the colliders of a new generation will have enough energy and luminosity integral to discover a Higgs boson unambiguously. We assume below that these efforts will be successful and discuss one of the subsequent series of problems.

Our point is: *The Higgs boson study provides the best way to probe New Physics effects with a scale  $\Lambda > 1$  TeV at lower energies.* Photon colliders ( $\gamma\gamma$  and  $\gamma e$ ) and hadron colliders (Tevatron and LHC) have an exceptional potential in this problem.

At energies below  $\Lambda$  the above New Physics effects would appear as some anomalous interactions of the particles already known. Since the  $\mathcal{SM}$  works well so far, we believe that almost in all cases these anomalies give rise only to small corrections to the  $\mathcal{SM}$  couplings, and consequently, they are hardly observable. Therefore, in our analysis we assume that main Higgs boson decay rates as well as the total Higgs boson width remain the same as in  $\mathcal{SM}$ . Oppositely, the Higgs boson interactions with photons ( $H\gamma\gamma$  and  $HZ\gamma$ ) or gluons ( $Hgg$ ) provide radically new opportunity since the correspondent  $\mathcal{SM}$  interactions arise only at the loop level. So, *the relative contribution of anomalous effects from underlying interactions will be enhanced in these vertexes.* This is the leading idea that motivates us to study processes<sup>1</sup>

$$\gamma\gamma \rightarrow H; \quad (1)$$

---

\*E-mail: ginzburg@math.nsc.ru

<sup>1</sup> The corresponding problems for the  $Hgg$  vertex extracted via the gluon fusion at Tevatron or LHC are studied elsewhere [1], [2].

$$\gamma\gamma \rightarrow HH; \quad (2)$$

$$\gamma e \rightarrow eH. \quad (3)$$

The reaction (1) was originally studied in this regard in refs. [3], the results were rederived in ref. [4]. The reaction (3) was analyzed in ref. [5], [6] for intermediate mass Higgs bosons.

In this paper we obtain more detailed results for the reaction (3) and present some conclusions from the comparative study of the two processes.

In principle, the same problem can be studied in process  $e^+e^- \rightarrow H\gamma$ . However, the cross section of this reaction is much lower (see e.g. [7]).

Throughout the paper, we work with the  $\mathcal{SM}$  Higgs boson. In accordance with modern LEP data we assume that  $M_H \gtrsim 90$  GeV [8]. In numerical calculations we set  $\sin^2\theta_W = 0.2315$ ,  $M_W = 80.3$  GeV,  $M_Z = 91.187$  GeV,  $M_t = 175$  GeV. We prefer to express results in terms of the Higgs field v.e.v.  $v$ , which is related to the Fermi coupling constant  $G_F$ , and use abbreviations:

$$\left(\sqrt{2}G_F\right)^{-1/2} = v = 246 \text{ GeV}, \quad c_W \equiv \cos\theta_W, \quad s_W \equiv \sin\theta_W. \quad (4)$$

Last,  $\lambda_i$  are the helicities of photons, and  $\zeta_e$  is the doubled electron helicity.

In the discussion below it is convenient to describe the  $H\gamma\gamma$  or  $HZ\gamma$  interaction via the effective lagrangians:

$$\mathcal{L}_{H\gamma\gamma} = \frac{G_\gamma}{2v} F^{\mu\nu} F_{\mu\nu} H, \quad \mathcal{L}_{HZ\gamma} = \frac{G_Z}{v} F^{\mu\nu} Z_{\mu\nu} H. \quad (5)$$

Here  $F_{\mu\nu}$  and  $Z_{\mu\nu}$  are the standard field strength tensors. Factor  $v^{-1}$  is introduced to make the effective coupling constants  $G_i$  (complex, generally speaking) dimensionless. The decay widths of Higgs boson are described via these  $G_i$  by relations

$$\Gamma_{H\rightarrow\gamma\gamma} = \frac{|G_\gamma|^2}{16\pi v^2} M_H^3, \quad \Gamma_{H\rightarrow Z\gamma} = \frac{|G_Z|^2}{8\pi v^2} M_H^3 \left(1 - \frac{M_Z^2}{M_H^2}\right)^3. \quad (6)$$

The values of these  $G_i$  in the  $\mathcal{MSM}$ — minimal  $\mathcal{SM}$  (with 1 Higgs doublet and 3 fermion generations) — are well known (see below (8), (9), (17) – (19)) [9]. In our case, the effects of New Physics can be reduced to some extra items in these  $G_i$ .

Usually, several effects of New Physics appear in the description of data simultaneously (for example, quadruple momentum and anomalous magnetic momentum of  $W$ , etc. in the reaction  $e^+e^- \rightarrow WW$ ). To separate out a particular anomaly from these effects is a difficult task. In our approach *a successive investigation of the reactions (1) and (3) allows one to study different anomalies independently.*

Future linear colliders are intended to be complexes operating in both  $e^+e^-$  mode and *Photon Collider* ( $\gamma e$  and  $\gamma\gamma$ ) modes with the following typical parameters (*which can be obtained without a specific optimization for the photon mode*) [10, 11] ( $E$  and  $\mathcal{L}_{ee}$  are the electron energy and luminosity at the basic  $e^+e^-$  collider.)

- *Characteristic photon energy*  $E_\gamma \approx 0.8E$ .
- *Annual luminosity*  $\mathcal{L}_{\gamma\gamma} \approx 0.3\mathcal{L}_{ee}$ , *typical*  $\mathcal{L}_{\gamma\gamma} = 100 \div 300 \text{ fb}^{-1}$ .

- Mean energy spread  $\langle \Delta E_\gamma \rangle \equiv \sqrt{\langle E_\gamma^2 \rangle - \langle E_\gamma \rangle^2} \approx (0.05 \div 0.07)E_\gamma$ .
- Mean photon helicity  $\langle \lambda_\gamma \rangle \approx 0.95$  with variable sign [10].
- Circular polarization of photons can be transformed into the linear one [12].

In other words, one can consider photon beams roughly monochromatic. For definiteness we use below  $\langle \Delta E_\gamma \rangle = 0.07E_\gamma$ .

The paper is organized as follows. In the next section we discuss processes (1)–(3) in the  $\mathcal{SM}$  with a special emphasis on the process  $e\gamma \rightarrow eH$ . In section 3 we explore anomalies and develop the effective lagrangian technique, which we then apply to our problem. A detailed investigation of new particles effects can also be found there. Finally, conclusions are drawn in section 4.

## 2 The production of the Higgs boson in the $\mathcal{MSM}$

In this section we assume the simplest variant of the  $\mathcal{SM}$  with 3 fermion generations.

Higgs coupling with photons arises due to triangle diagrams with circulating quarks, charged leptons or  $W$ -bosons. The natural scale of the above effective couplings  $G_i$  is given by the fine structure constant  $\alpha$ . So, we define

$$G_\gamma^{SM} = \frac{\alpha\Phi_\gamma}{4\pi}, \quad G_Z^{SM} = \frac{\alpha\Phi_Z}{4\pi}. \quad (7)$$

$$\Phi_\gamma = \Phi_\gamma^1(r_W) + \sum_f N_c Q_f^2 \Phi^{1/2}(r_f), \quad r_P = \frac{4m_P^2}{M_H^2}, \quad (8)$$

$$\Phi_\gamma^1 = 2 + 3r - 3r(2-r)\phi^2(r), \quad \Phi^{1/2} = -2r[1 - (1-r)\phi^2(r)];$$

$$\phi(r) = \begin{cases} -i \arcsin \frac{1}{\sqrt{r}} & \text{at } r > 1; \\ \ln \left( \frac{1 + \sqrt{1-r}}{\sqrt{|r|}} \right) - \frac{i\pi}{2}\theta(r) & \text{at } r < 1. \end{cases} \quad (9)$$

The corresponding quantities for the off-shell photon or Z are written below (17)–(19). For the considered Higgs boson mass interval, the main contribution is given by the  $W$ -boson and  $t$ -quark loops.

The mass shell values of  $|\Phi_\gamma|$ ,  $|\Phi_Z|$  with their real and imaginary parts are shown in Fig. 1. One can see that  $|\Phi_\gamma|$  is about  $5 \div 10$  for  $M_H < 350$  GeV and  $Re\Phi_\gamma$  changes its sign at  $M_H \approx 350$  GeV (due to a compensation between  $t$ -quark and  $W$ -boson loops). The quantity  $\Phi_Z$  is typically larger than  $\Phi_\gamma$  by a factor about 2.

### 2.1 Higgs boson production in $\gamma\gamma$ collisions

#### $\gamma\gamma \rightarrow H$ process

The most important process here is the resonant Higgs boson production,  $\gamma\gamma \rightarrow H$ . Since this process has been studied in literature well enough, we briefly review the main results.

Describing the luminosity distribution near its peak by the Lorencian form, one obtains the cross section of the Higgs boson production averaged over the luminosity distribution:

$$\langle \sigma \rangle = \int \sigma(\sqrt{s}) \frac{1}{\mathcal{L}_{\gamma\gamma}} \frac{d\mathcal{L}_{\gamma\gamma}}{d\sqrt{s}} d\sqrt{s} \equiv 8\pi (1 + \lambda_1 \lambda_2) \frac{\Gamma_{H \rightarrow \gamma\gamma}}{M_H^3} Br(H \rightarrow A) \frac{M_H}{\Gamma_H + \Delta E_\gamma}. \quad (10)$$

Here  $Br(H \rightarrow A)$  is the branching ratio of the Higgs boson decay into a particular channel  $A$ .

Depending on the value of  $M_H$ , different final states should be used for the Higgs boson exploration ( $b\bar{b}$  for  $M_H < 140$  GeV,  $W^*W$  at  $120 \text{ GeV} < M_H < 190$  GeV,  $ZZ^*$  and  $ZZ$  at  $M_H > 140$  GeV, etc.). The cross sections of the Higgs boson production for the most important channels are plotted in Fig. 2. (For more detailed description see refs. [13] – [16].)

### $\gamma\gamma \rightarrow HH$ process

Of special interest is the process  $\gamma\gamma \rightarrow HH$ . In ref. [17] the explicit calculation of this reaction was performed at one-loop level and a detailed analysis was carried out. At  $\sqrt{s} < 1$  TeV the total cross section of this reaction is less than 1 fb, i. e. virtually negligible. This cross section exhibits a remarkable growth with both  $s$  and  $M_H$  increasing almost up to the kinematical limit, it is about few fb for  $\sqrt{s} = 2$  TeV,  $M_H = 0.8$  TeV.

## 2.2 $e\gamma \rightarrow eH$ process

We discuss the  $e\gamma \rightarrow eH$  process at c.m.s. energy squared  $s \gg M_H^2$ . Besides, we have in mind the experiments with recording of a scattered electron having transverse momentum  $p_\perp \geq p_{\perp 0}$  which is related to the variable  $Q^2 \equiv -(p_e - p'_e)^2$  as

$$p_\perp^2 = Q^2 \left( 1 - \frac{M_H^2 + Q^2}{s} \right), \quad Q^2 \geq Q_{min}^2 = \frac{m_e^2 M_H^4}{s(s - M_H^2)} \quad (11)$$

The cross section of this reaction is obviously less than that of the reaction (1). Therefore it cannot be considered as a new source of Higgs bosons themselves. In addition to the new test of  $\mathcal{SM}$ , *a novel feature of this process is the possibility to study  $Z\gamma H$  coupling*. So, concerning this reaction, our main goal is to extract information about this interaction.

The cross section of this process in the equivalent photon approximation was calculated in refs. [18, 19]. Recently this process has been considered in detail in ref. [5] for light Higgs boson ( $80 < M_H < 140$  GeV) with  $H \rightarrow b\bar{b}$  decay channel (and in ref. [20] without detailed analysis<sup>2</sup>). It was shown that this process is helpful to study  $\gamma ZH$  interaction. Here we consider this process in more detail and for a wider region of the Higgs boson masses.

**Different contributions and gauge invariance.** We discuss the amplitude of the physical process, that is the projection of a calculated amplitude on mass shell states. We assume this procedure when decomposing an amplitude into several parts. (This projection does not affect the whole amplitude but it changes separate items.) It means, in particular, that all items longitudinal in external photon momentum  $k$  are removed from each contribution in this projection.

---

<sup>2</sup> Note obvious misprints in formulas (7), (8), (21) in ref. [20].

This amplitude can be written as a sum of three items. The first one,  $\mathcal{A}_\gamma$ , is the  $\gamma$ -pole exchange contribution (photon exchange between scattered electron and triangle loop describing  $\gamma^*\gamma \rightarrow H$  subprocess). This item is evidently gauge-invariant since longitudinal item in photon propagator gives in the electron vertex  $q^\mu u(p')\gamma^\mu u(p) \rightarrow u(p')(\hat{p}-\hat{p}')u(p) = 0$ . The second item is the  $Z$ -pole exchange contribution  $\mathcal{A}_Z$  ( $Z$ -boson exchange between scattered electron and triangle loop describing  $Z^*\gamma \rightarrow H$  subprocess). This item is *approximately* gauge-invariant with accuracy  $\sim m_e/M_Z$ . Indeed, the gauge dependent longitudinal item in propagator gives in the electron vertex

$$\frac{q^\mu}{M_Z}\bar{u}(p')\gamma^\mu(v+a\gamma^5)u(p) \rightarrow \frac{1}{M_Z}\bar{u}(p')(\hat{p}-\hat{p}')(v+a\gamma^5)u(p) = 2a\frac{m_e}{M_Z}\bar{u}(p')\gamma^5u(p).$$

The residual item (we denote it as box<sup>3</sup>) is, consequently, gauge-invariant with this very accuracy<sup>4</sup>. Having in mind a perturbative accuracy not better than  $\alpha \gg m_e/M_Z$ , we consider the above subdivision into 3 items gauge invariant.

The box item can in turn be split into  $W$  and  $Z$ -boson contributions (denoted as  $W$  and  $Z$ ) in respect to  $W$  or  $Z$  bosons circulating in loops.

In these terms the cross section of reaction for the pure initial helicity states  $\lambda_\gamma = \pm 1$ ,  $\zeta_e = \pm 1$  can be written as ( $s$  and  $u$  are usual Mandelstam variables)

$$\frac{d\sigma}{dQ^2} = \frac{1}{64\pi s^2} \frac{\alpha^4 M_W^2 Q^2}{\sin^6 \theta_W} \cdot \left[ s^2(1 + \lambda_\gamma \zeta_e) |\mathcal{A}_\gamma + \mathcal{A}_Z + Z(s, u) + W(s, u)|^2 + u^2(1 - \lambda_\gamma \zeta_e) |\mathcal{A}_\gamma + \mathcal{A}_Z + Z(u, s) + W(u, s)|^2 \right]. \quad (12)$$

**Qualitative analysis.** The total cross section of the process is estimated in spirit of Equivalent Photon Approximation, it is about  $(\alpha/\pi) \ln[s^2/(m_e^2 M_H^2)] \sigma_{\gamma\gamma \rightarrow H} \sim (10 \div 20)$  fb (see Fig. 3). It is remarkable that effects of  $\gamma ZH$  interaction are about several fb and seem to be observable.

For a better understanding of the reaction, let us discuss the magnitude of separate contributions for different  $Q^2$  values. Let us note that a typical box contribution is  $\propto 1/s$  whereas triangle effective couplings  $\Phi_i$  are  $s$  independent and depend on  $Q^2$  smoothly at  $Q^2 < M_H^2$ . So, at  $Q^2 \ll s$  both  $\mathcal{A}_\gamma$  and  $\mathcal{A}_Z$  contributions are enhanced due to small propagator denominators  $1/Q^2$  or  $1/(Q^2 + M_Z^2)$ . This enhancement in cross section is compensated partly by a (diffractive) factor  $\sim Q^2$  in  $e\bar{e}\gamma$  or  $e\bar{e}Z$  vertices. Nevertheless, these items give the dominant contribution in the total cross section with the enhancement factor  $\sim \ln(M_H^2/Q_{min}^2)$  for  $|\mathcal{A}_\gamma|^2$  and  $\sim \ln(M_H^2/M_Z^2)$  for  $|2Re\mathcal{A}_\gamma^*\mathcal{A}_Z + \mathcal{A}_Z^2|$ . At  $Q^2 \ll M_Z^2$  and, consequently, in the total cross section photon contribution strongly dominates. With the growth of  $Q^2$  up to values comparable with  $M_Z^2$ , the contribution  $|2Re\mathcal{A}_\gamma^*\mathcal{A}_Z + \mathcal{A}_Z^2|$  becomes competitive with  $|\mathcal{A}_\gamma|^2$ . Finally, at  $Q^2 \sim s$  the box contribution becomes sizable too. Its relative contribution to the total cross section is less than  $Z$ -pole diagram by a factor  $\sim M_H^2/s$  with no large logarithms.

As far as we are interested in extraction of  $\gamma ZH$  interaction, we deduce from the above discussion that the  $Z$ -exchange contribution grows relatively in the cross section,

<sup>3</sup> It is a sum of box diagrams themselves and relevant  $s$ - and  $u$ -pole diagrams.

<sup>4</sup> Similar subdivision without projection for the mass shell states is gauge dependent, see [7], the items that violated gauge invariance in that approach disappear in the matrix element considered.

integrated over the region  $p_\perp > p_{\perp 0}$  with large enough  $p_{\perp 0}$ :

$$\sigma(Q_0^2) = \int_{Q_0^2}^{s-M_H^2-Q_0^2} \frac{d\sigma(Q^2)}{dQ^2} dQ^2, \quad (13)$$

where quantity  $Q_0^2$  is related to the  $p_{\perp 0}$  via eq. (11). The upper limitation here describes elimination of small transverse momenta of electrons scattered in backward direction.

In the cross section (13) the pole contributions are approximately independent from energy since integral over  $Q^2$  converges practically at  $Q^2 \sim M_H^2$ , which is the scale of decreasing of triangle loop itself with the growth of  $Q^2$ . Simultaneously, box contribution decreases with  $s$  growth.

The second step in extracting of  $\gamma ZH$  vertex is to consider and compare the cross sections  $d\sigma_L$  and  $d\sigma_R$  for the left hand and right hand polarized electrons. In a qualitative analysis one can neglect box contributions and express these cross sections in terms of vector  $M_V$  and axial amplitudes  $M_A$ . The axial amplitude  $M_A$  utterly originates from the  $Z$  boson exchange ( $J^Z$ ), whereas the vector amplitude receives contributions from both photon and  $Z$  boson:

$$M_V = \frac{1}{Q^2} J^\gamma + \frac{1/4 - \sin^2 \theta_W}{Q^2 + M_Z^2} J_V^Z; \quad M_A = \frac{1}{Q^2 + M_Z^2} J_A^Z. \quad (14)$$

(Since  $1/4 - \sin^2 \theta_W \ll 1$ ,  $M_V \propto J^\gamma$  with good accuracy.)

With this notation,  $d\sigma_{L,R} \propto |M_V \pm M_A|^2$ . Therefore the difference between these cross sections  $\Delta\sigma$  and the cross section for the unpolarized electrons  $\sigma^{np}$  are

$$\Delta d\sigma \equiv d\sigma_L - d\sigma_R \propto \text{Re}(M_V^* M_A), \quad d\sigma^{np} \equiv \frac{d\sigma_L + d\sigma_R}{2} \propto (|M_V|^2 + |M_A|^2). \quad (15)$$

In other words, the quantity  $\Delta\sigma$  directly reveals the magnitude of  $\gamma Z^* H$  interaction.

To see the role of the initial photon helicity in this process, it is instructive to recall that a longitudinally polarized electron transmits a part  $x = M_H^2/s$  of its polarization to an exchanged photon [21]. The same is also valid for an exchanged  $Z$ -boson. On the other hand, a Higgs boson can be produced only in the total spin zero state. Therefore, choosing an appropriate photon polarization, one can affect the rate of the Higgs boson production in  $e\gamma$  collisions. It is clear that this influence will decrease with  $s/M_H^2$  growth.

**Details of calculations.** In our calculations we used corrected formulas<sup>5</sup> from ref.[7] (obtained for the  $e^+e^- \rightarrow H\gamma$  process) after transforming them for our kinematical region. The result is expressed in terms of standard scalar loop integrals.

The pole contributions are written as sums of triangle diagrams for which integration can be performed analytically. These contributions can be written via the  $Q^2$  dependent functions  $\Phi_i$  defined in eqs. (5), (7) as

$$\mathcal{A}_\gamma = \frac{s_W^2}{Q^2 M_W^2} \Phi_\gamma, \quad \mathcal{A}_Z = \frac{s_W}{4c_W(Q^2 + M_Z^2)M_W^2} \Phi_Z. \quad (16)$$

---

<sup>5</sup> Note that in ref.[7] the fermion contribution in formulas (12), (13) should be twice larger.

The functions  $\Phi_i$  are split into the fermion and  $W$ -boson parts:

$$\begin{aligned}\Phi_\gamma &= \sum_f N_c Q_f^2 \Phi^{1/2}(f) + \Phi_\gamma^1(W); \\ \Phi_Z &= \sum_f N_c Q_f v_f \Phi^{1/2}(f) + \Phi_Z^1(W); \quad v_f = \frac{I_f - 2Q_f s_W^2}{2c_W s_W}.\end{aligned}\tag{17}$$

Turning from  $\Phi_\gamma$  to  $\Phi_Z$ , one observes that the fermion contribution is modified merely by a replacement of the appropriate 'charges' whereas  $W$ -boson undergoes more serious transformation. These contributions can be written via loop integrals with function  $\phi$  defined in (9) and quantity  $w = Q^2/M_H^2$  as:

$$\begin{aligned}\Phi^{1/2}(f) &= -\frac{2r_f}{1+w} [C_{23}(w, r_f) - C_0(w, r_f)]; \\ \Phi_\gamma^1(W) &= \frac{1}{1+w} [(3r_w + 2)C_{23}(w, r_w) - 8r_w C_0(w, r_w)]; \\ \Phi_Z^1(W) &= \left(\frac{c_W}{s_W} - \frac{1}{4c_W s_W}\right) \Phi_\gamma^1 - \frac{(2 - r_w)C_{23}(w, r_w)}{4s_W c_W (1+w)}.\end{aligned}\tag{18}$$

$$\begin{aligned}C_0(w, r) &= \phi^2(r) - \phi^2\left(-\frac{r}{w}\right), \\ C_{23}(w, r) &= 1 + \frac{r}{1+w} C_0(w, r) + \frac{2w}{1+w} \left[ \sqrt{1-r} \phi(r) - \sqrt{1+\frac{r}{w}} \phi\left(-\frac{r}{w}\right) \right],\end{aligned}\tag{19}$$

with  $\sqrt{1-r} = +i\sqrt{r-1}$  at  $r > 1$ .

Setting  $Q^2$  to zero ( $w = 0$ ), one obtains mass shell value of  $\Phi_\gamma$  (8).

The box items can be written down via a number of dilogarithms of distinct arguments. Since their contribution to cross sections are rather small, we give all relevant formulas in Appendix (provided only for the hep-ph version of this paper).

These equations are rather complicated. So, we performed several checks to verify the expressions used in our calculations. First, we checked numerically the consistency of analytical formulas for scalar loop integrals. For this purpose we compared numbers obtained from our formulas and those obtained with FF package [22]. We found that at a typical phase space point the two approaches give coincident results for all loop integrals up to 9 significant digits or better. Besides, we examined the behavior near the points  $Q^2, u = 0$  of the box contribution decomposed into several scalar loops terms. It is clear that there is no physical singularity at these points, so the results must remain stable here. Indeed, near these points we observed some 8 digits cancelation among these terms, which allowed the box contribution to remain virtually constant down to  $Q^2, |u| \sim 0.01$  GeV<sup>2</sup>. However, for significantly lower values of  $Q^2, |u|$  both our formulas and FF package yield numerically unstable results due to computer precision limitations.

Second, comparing different contributions separately, we found complete agreement with corrected results of [5].

**Main radiative corrections.** We start our calculations from value  $\alpha(0) = 1/137$  which is the fine structure constant for the real photon independent from its energy. The identical electric charge in all electromagnetic vertices is necessary to have gauge invariant QED and in other vertices to have EW gauge invariance.

There are two types of radiative corrections for the process discussed. First, there are radiative corrections related to the photon emission etc. from virtual heavy particles.

They are  $\sim \alpha$  and can be omitted at our 1 percent level of accuracy. The second type is represented by large (logarithmic) radiative corrections connected with light particles only. Those are  $e^+e^-$ ,  $\mu^+\mu^-$ , etc. loops in the propagators of photon or  $Z$  and similar  $e\nu$ , etc. loops in  $W$  propagator. Their effect could be accounted by the change  $\alpha(0) \rightarrow \alpha(Q^2)$ . Since  $Q^2 \sim M_Z^2$  in our case, we change  $\alpha(0) = 1/137$  to  $\alpha(M_Z^2) = 1/128$  in 2 vertices of diagrams where neither real photon nor Higgs boson is involved.

With the same accuracy both initial state radiation (ISR) and final state radiation (FSR) of electron should be taken into account. There are two effects essential for our study. The first one is an effective decreasing of initial electron energy (decreasing of  $s$ ) due to ISR. The second effect is the smoothing of result over some interval of  $Q^2$  since observed transverse momentum of electron  $p_{\perp,exp}$  differs from "true" one due to emission of photon in FSR.

Fortunately, ISR + FSR work weakly in our case. Indeed, the cross sections (13) has only a slight dependence<sup>6</sup> on  $s$ . Next, the effect of difference between true  $p_{\perp}$  and  $p_{\perp,exp}$  becomes small at the calorimetric method of electron momentum recording. In this case the final radiative correction becomes not so large. Anyway, this effect depends strongly on the method of recording of a scattered electron and it can be taken into account in more detailed simulation only.

**Discussion of numeral results.** The exact calculations confirm the above qualitative analysis. Some numerical data with different contributions can be found in Table 1. A detailed analysis of the numbers obtained shows that the pole contributions in  $\sigma(Q^2)$  become practically independent from  $s$  already at the moderate energy, whereas box contributions and the cross sections difference for opposite initial photon helicities decrease with  $s$  growth. With growth of  $Q_0^2$ , the photon contribution is reduced whereas  $Z$  contribution has only a weak dependence on  $Q_0$  unless  $Q_0^2 \gtrsim M_Z^2$ . This behavior is clearly seen in Table 2, where  $\sigma^{np}$  and  $\Delta\sigma$  are given for various  $Q^2$  cut-off. Last, the box items contribute less than 0.1 *fb* to the total cross section at the considered energies.

These results are summarized in Fig.4, where various dependencies for the cross sections are presented.

*The conclusions:*

- The  $e\gamma \rightarrow eH$  process is observable for wide enough interval of Higgs boson masses and with large enough  $Q_0^2$  for different polarizations of colliding particles.
- The  $\gamma Z$ -interference term is strongly enhanced for the polarized cross sections. The effect of  $\gamma ZH$  interaction becomes relatively large even at  $p_{\perp} > 10$  GeV.
- The contribution of  $Z$ -pole exchange is saturated at  $Q^2 = Q_0^2 > 1000$  GeV<sup>2</sup>. It decreases slowly with  $Q_0^2$  growth up to  $M_Z^2$ . The values of  $\sigma_{L,R}(Q^2)$  at  $Q_0^2 \geq 1000$  GeV<sup>2</sup> depend weakly on  $s$ .
- The measurements of polarized cross sections at  $p_{\perp} > p_{\perp,0}$  with  $p_{\perp,0} = (10 \div 50)$  GeV provides an opportunity to extract virtually complete information about  $\gamma ZH$  vertex without any reduction of **useful** statistics.
- If  $M_H < 300$  GeV, the increase of c. m. energy above 500 GeV would not lead to any significant improvement in statistics. It means, in particular, that initial photon energy spread and shift of energy of exchanged photon or  $Z$  affect the final results weakly.

---

<sup>6</sup> It is in contrast with the total cross section which depends on  $s$  mainly via contribution of very small  $Q^2$  near  $Q_{min}^2$ . This contribution is absent in the cross sections  $\sigma(Q_0^2)$ .



### 3 Higgs boson anomalous interaction

#### 3.1 The Effective Lagrangian

Assuming that at very small distances some New Physics comes into play, one can consider the Standard Model as the low energy limit of this yet unknown theory with a characteristic scale of new phenomena  $\Lambda > 1$  TeV. At energies below  $\Lambda$  this underlying theory manifests itself as some anomalous interactions (*anomalies*) of known particles. These interactions can be described by means of an effective lagrangian which is written as expansion<sup>7</sup> in  $\Lambda^{-1}$ :

$$L_{eff} = L_{SM} + \sum_{k=1}^{\infty} \Delta L_k; \quad L_{SM} = -\frac{B_{\mu\nu}B^{\mu\nu}}{4} - \frac{W_{\mu\nu}^i W^{i\mu\nu}}{4}, \quad \Delta L_k = \sum_r \frac{d_r \mathcal{O}_r^k}{\Lambda^k}. \quad (20)$$

Here  $L_{SM}$  is the lagrangian of the Standard Model and the dimension of operators  $\mathcal{O}_r^k$  is  $4 + k$ . Here, as usual,

$$B_{\mu\nu} = \partial_\mu B_\nu - \partial_\nu B_\mu, \quad W_{\mu\nu}^i = \partial_\mu W_\nu^i - \partial_\nu W_\mu^i - g\epsilon^{ijk}W_\mu^j W_\nu^k.$$

Besides, the covariant derivative for a weak isospin doublet with hypercharge  $Y = 1/2$  is defined as

$$D_\mu = \partial_\mu + \frac{i}{2}g'B_\mu + ig\frac{\tau^i}{2}W_\mu^i.$$

It is usually assumed that the symmetry of  $L_{eff}$  is the same as that of  $L_{SM}$ . For this case it is known that  $\Delta L_1 = 0$ . Therefore, we consider the next largest term  $\Delta L_2$ . The whole set of dimension–six operators that can appear in  $\Delta L_2$  is given in refs. [23, 24, 25]. Only five of them are relevant to our problem [25], i. e. give rise to anomalous  $\gamma\gamma H$  or  $\gamma ZH$  interactions. They can be written as

$$\begin{aligned} \mathcal{O}_{BB} &= \phi^+ B_{\mu\nu} B^{\mu\nu} \phi; & \mathcal{O}_{WW} &= \phi^+ W_{\mu\nu}^i W^{i\mu\nu} \phi; \\ \mathcal{O}_{BW} &= \phi^+ B_{\mu\nu} \tau^i W^{i\mu\nu} \phi; & & \\ \mathcal{O}_B &= i(D_\mu \phi)^+ B^{\mu\nu} (D_\nu \phi); & \mathcal{O}_W &= i(D_\mu \phi)^+ \tau^i W^{i\mu\nu} (D_\nu \phi). \end{aligned} \quad (21)$$

Note that all operators here are Hermitian.

The standard transformation of  $\mathcal{SM}$  conserves only the neutral component of the doublet:  $\phi = (0, \frac{v+H}{\sqrt{2}})$ . (Other components are converted into longitudinal components of  $W, Z$ ). In other words, we should replace

$$(\phi^+ \phi) = (H^2 + 2Hv + v^2)/2; \quad (\phi^+ \tau^i \phi) = -(H^2 + 2Hv + v^2)\delta_{i3}/2.$$

After that we consider only the part of  $\Delta L_2$  resulting from operators (21). We consider two items from this part.

The first one is that with gauge fields but without Higgs field operators. That is

$$\Delta L_{(0)} = \frac{v^2}{2\Lambda^2} \left( d_{BB} B_{\mu\nu} B^{\mu\nu} + d_{WW} W_{\mu\nu}^i W^{i\mu\nu} - d_{BW} B_{\mu\nu} W^{3\mu\nu} \right).$$

---

<sup>7</sup> For the observable effects it means expansion in  $(E/\Lambda)$ .

(The operators  $\mathcal{O}_B$  and  $\mathcal{O}_W$  do not contribute here since they are proportional to the derivative of the Higgs field.)

The first two terms here are absorbed in  $L_{SM}$  after simple renormalization of the fields  $W^{i\mu} \rightarrow W^{i\mu}(1 - 2d_{WW}v^2/\Lambda^2)^{1/2}$ ;  $B^\mu \rightarrow B^\mu(1 - 2d_{BB}v^2/\Lambda^2)^{1/2}$ . Therefore, they give no observable effects. Oppositely, the last term in  $\Delta L_{(0)}$  introduces an additional  $B - W^3$  mixing and thus changes the value of the Weinberg angle. Therefore some constraints on  $d_{BW}$  from the data can be written out [25].

The second item of interest describes nonstandard interactions of a Higgs boson with gauge bosons. Going from fields  $W^3$  and  $B$  to the physical fields  $A$  and  $Z$ , one immediately reveals that anomalous  $\gamma\gamma H$  and  $\gamma ZH$  interactions arising from all five operators are of *the same pattern*. All these contributions can be summarized in the expression:

$$\Delta L_v = (2Hv + H^2) \left( \theta_\gamma \frac{F_{\mu\nu} F^{\mu\nu}}{2\Lambda_\gamma^2} + \theta_Z \frac{Z_{\mu\nu} F^{\mu\nu}}{\Lambda_Z^2} \right), \quad (\theta_i = \pm 1). \quad (22)$$

Here we introduced  $\Lambda_i$  by

$$\frac{\theta_\gamma}{\Lambda_\gamma^2} = \frac{1}{\Lambda^2} (s_W^2 d_{WW} + c_W^2 d_{BB} - c_W s_W d_{WB}),$$

$$\frac{\theta_Z}{\Lambda_Z^2} = \frac{1}{2\Lambda^2} \left[ \sin 2\theta_W (d_{WW} - d_{BB}) - \cos 2\theta_W d_{WB} + \frac{\bar{g}}{4} (d_W - d_B) \right]; \quad \bar{g}^2 \equiv g^2 + g'^2.$$

To shorten the description of results, we will write sometimes a quantity  $\tilde{\Lambda}_i \equiv \theta_i \Lambda_i$  instead of  $\Lambda_i$  and  $\theta_i$  separately.

In the detailed treatment of our processes with the  $\mathcal{SM}$  contribution these anomalies correspond to the change in (5), (7)

$$G_i = G_i^{SM} + \Delta G_i \equiv \frac{\alpha}{4\pi} (\Phi_i + \Delta\Phi_i) \Rightarrow G_\gamma = \frac{\alpha}{4\pi} \Phi_\gamma + \frac{\theta_\gamma v^2}{\Lambda_\gamma^2}, \quad G_Z = \frac{\alpha}{4\pi} \Phi_Z + \frac{\theta_Z v^2}{\Lambda_Z^2}. \quad (23)$$

The residual items of  $\mathcal{L}_{eff}$  describe anomalous interaction of Higgs field with  $W$  or  $Z$  bosons. They should be considered in the context of quite different experiments. The observation of anomalies of this type is more difficult since they appears in interactions where the  $\mathcal{SM}$  couplings occur at the tree level.

The two-parametric form (22) is the final form which can be used for the discussion of considered experiments. The separate information about different parameters  $d_r$  can be obtained only if one has some additional information about their interrelation (either in some separate theory or using experimental data related to the  $HWW$  and  $HZZ$  anomalies). In principle, aside from written above terms, the anomaly  $H^2 F_{\mu\nu} F^{\mu\nu}$  can appear from items which do not contain linear in Higgs field parts. However, these new items originate from operators of 8-th order in  $L_{eff}$ . Therefore, their natural magnitude is  $v^4/\Lambda^4$  and we neglect them.

Possible  $\mathcal{CP}$  violating terms in the anomalous interactions constitute a special problem. It will be discussed separately.

### 3.2 Simplest variant of New Physics — new heavy particles within $\mathcal{SM}$

The simplest variant of New Physics is "trivial" extension of  $\mathcal{SM}$  with introduction of new heavy generations of quarks of leptons  $f'$  (modern data does not forbid existence

of such extra generations having heavy neutrinos with mass  $m_\nu > 45$  GeV) or some additional heavy  $W'$  bosons. In the context of  $\mathcal{SM}$  the Yukawa coupling constants of these new particles with Higgs boson are proportional to their masses  $M_i$ . Therefore, there is no decoupling in the interactions of Higgs boson induced by these new particles in intermediate states. In particular, the loops for the  $H\gamma\gamma$ ,  $HZ\gamma$  and  $Hgg$  interactions are left finite at  $M_i^2 \gg M_H^2, Q^2$  [9].

The corresponding new items in an effective lagrangian are calculated easily with the aid of eqs. (17)–(19), (9) for both variants of new heavy gauge charged vector boson ( $W'$ ) or one extra generation of heavy quarks and leptons<sup>8</sup> ( $f'$ ):

$$\Delta\Phi_\gamma(W') = 7, \quad \Delta\Phi_Z(W') = \frac{31 - 42s_W^2}{6s_W c_W} \approx 8.41; \quad (25)$$

$$\Delta\Phi_\gamma(f') = -32/9, \quad \Delta\Phi_Z(f') = -4\frac{3 - 8s_W^2}{9s_W c_W} \approx -1.21. \quad (26)$$

These quantities are so large (compare them with Fig. 1) that they change dramatically  $\gamma\gamma H$  and  $\gamma ZH$  couplings (as well as  $ggH$  interaction). It leads to strong departures in corresponding decay widths and production cross sections.

Let us discuss corresponding variations in the processes considered in more detail.

*Photon collisions,  $\gamma\gamma \rightarrow H$  (Fig. 5).*

New vector boson gives rise to a dramatic enhancement of this cross section throughout the whole range of the Higgs boson mass. In this case the cross section enhances by a factor  $3 \div 100$ .

The fourth fermion generation causes a destructive effect for  $M_H < 300$  GeV, but also enlarges the rate of Higgs boson production for higher values of  $M_H$ . This generation changes cross section by a factor  $0.2 \div 50$  depending on the Higgs boson mass. Note that these particles enable the Higgs boson to be observable in the reaction (1) at  $M_H > 400$  GeV (where this observation is doubtful with the standard set of particles).

These effects are strong, therefore one can consider the Higgs boson two-photon width as a counter of the number of new particles heavier than the Higgs boson within  $\mathcal{SM}$ .

*Photon collisions,  $\gamma\gamma \rightarrow HH$ .*

Let us assume that the masses of discussed heavy particles  $M_i$  are so large that  $M_i^2 \gg s > 4M_H^2$ . In this case the additional items to the amplitudes calculated in ref. [17] are written in the form of  $\gamma\gamma HH$  item in eq. (22) and coupling constants (25), (26). Therefore, the considered anomalous Higgs boson production in  $\gamma\gamma \rightarrow H$  reaction should be accompanied by a deviation of  $HH$  production rate in the process  $\gamma\gamma \rightarrow HH$ . Similar opportunity was studied first in ref. [3].

Neglecting small  $\mathcal{SM}$  contribution, one has two diagrams for this reaction from interaction (22), the pointlike one and  $\gamma\gamma \rightarrow H \rightarrow HH$ . Provided  $H^3$  vertex is the same as

---

<sup>8</sup> In terms of effective lagrangian (22) and eq. (23) these very quantities correspond to

$$\begin{aligned} \tilde{\Lambda}_1(W') &= 5.4 \text{ TeV}, & \tilde{\Lambda}_2(W') &= 4.9 \text{ TeV}; \\ \tilde{\Lambda}_1(f') &= 7.6 \text{ TeV}, & \tilde{\Lambda}_2(f') &= 13 \text{ TeV}. \end{aligned} \quad (24)$$

Note also that the entire fermion generation contribution in  $\Delta\Phi$  written above is twice as large as  $t'$ -quark contribution.

in  $\mathcal{SM}$ , the resulting cross section for  $\gamma\gamma$  collisions with the total initial state helicity 0 ( $\lambda_1\lambda_2 = 1$ ) is:

$$\sigma_{\gamma\gamma\rightarrow HH} = \frac{s}{8\pi\Lambda_\gamma^4} \sqrt{1 - \frac{4M_H^2}{s}} \cdot \left( \frac{s + 2M_H^2}{s - M_H^2} \right)^2 \approx 62 \text{ pb} \cdot \frac{s(\text{TeV}^2)}{\Lambda_\gamma^4}. \quad (27)$$

The last approximation is valid just above the threshold. The angular distribution of produced  $H$  is roughly isotropic.

In particular, the existence of new heavy  $W'$  or fourth generation in  $\mathcal{SM}$  gives the cross sections

$$\sigma_{\gamma\gamma\rightarrow HH}(W') \approx 73 \text{ fb} \cdot s(\text{TeV}^2), \quad \sigma_{\gamma\gamma\rightarrow HH}(f') \approx 19 \text{ fb} \cdot s(\text{TeV}^2). \quad (28)$$

The effect appears observable regardless of the Higgs boson mass.

*Electron-photon collisions,  $e\gamma \rightarrow eH$ .* Fig. 6 represents the effect of new heavy particles on  $e\gamma \rightarrow eH$  cross sections. It is seen that the effect of modified  $ZH\gamma$  coupling is extremely large in the case of a heavy gauge vector boson and it is large for new heavy particles from the fourth generation.

*Notes about Higgs boson production at Tevatron and LHC [1].* The main mechanism of the Higgs boson production at hadron colliders is gluon fusion. The Higgs boson coupling with gluons (similar to (5)) arises from triangle diagrams with circulating quarks only. This effect is described by quantity  $\Phi_g^{1/2}$  (8) whose absolute value is shown at Fig. 1. The major contribution is given by  $t$ -quark loop. An additional new gauge boson  $W'$  does not influence this effective coupling while adding of a new fermion generation would increase this coupling by a factor about 3. It results in a tremendous growth of the Higgs boson production cross section by a factor  $6 \div 9$  (depending of  $M_H$ ). This effect may be seen in the forthcoming experiments at the upgraded Tevatron by looking for an excess of  $\tau^+\tau^-$  events for  $M_H < 150$  GeV and it will be clearly observed in all decay channels at LHC.

Therefore, effects of new heavy particles in  $\mathcal{SM}$  are observable very well in all channels discussed. However in some particular channels similar effects might also be brought about by completely different causes. For instance, the modification of  $H\gamma\gamma$  effective coupling caused by fourth generation can be mimicked in the two Higgs doublet model with some relations among free parameters of the model. However, the probability of this "miraculous" imitation seems extremely small if one observes the whole set of effects in all the production channels just discussed.

### 3.3 General anomalies

Let us consider the case when effects of New Physics have another nature, e. g. SUSY, Technicolour, etc. but there are no new heavy particles within the  $\mathcal{SM}$  sector. In this case, the scale of new effects is given by parametrization (22). These effects for the processes  $\gamma\gamma \rightarrow H$  and  $\gamma\gamma \rightarrow HH$  were considered first in ref. [3] (neglecting interference with  $\mathcal{SM}$  result). More detailed treatment of process  $\gamma\gamma \rightarrow H$  with taking into account the interference with  $\mathcal{SM}$  quantities was performed in ref. [4] in the relatively narrow

region of  $M_H$ . These anomalies for the process  $e\gamma \rightarrow eH$  were considered in ref. [6] for  $M_H \leq 140$  GeV.

As we have seen, new particles within  $\mathcal{SM}$  resulted in large effects on  $\gamma\gamma \rightarrow H$  and  $e\gamma \rightarrow eH$  cross sections. These effects correspond to large enough scales (24). One can expect that the *ultimate* values of  $\Lambda_i$  which can be experimentally analyzed will be even higher.

Let us note that the sensitivity of process (1) to the  $\Lambda_\gamma$  is much higher than that of process (3). Indeed, the observed cross section in the latter case is lower than that in the  $\gamma\gamma$  collision. The same physical backgrounds is unavoidably transferred to the  $\gamma e$  case (with corresponding reduction of effective luminosity). For example, background  $\gamma\gamma \rightarrow b\bar{b}$  turns into  $\gamma e \rightarrow e b\bar{b}$  with two photon mechanism of  $b\bar{b}$  pair production. Moreover, an additional backgrounds could arise in  $\gamma e$  collisions, such as  $\gamma e \rightarrow e b\bar{b}$  with one photon (bremsstrahlung) mechanism of  $b\bar{b}$  pair production.

Therefore, *the process (1) should be used for derivation of  $\Lambda_\gamma$ , and then  $\Lambda_Z$  should be extracted from the process (3) provided  $\Lambda_\gamma$  is known.* Thus, we separate these effects and investigate the reaction  $\gamma e \rightarrow eH$  with no  $H\gamma\gamma$  anomaly. When  $H\gamma\gamma$  anomaly is known, this effect can be easily taken into account. The  $H\gamma\gamma$  anomaly often enhances the effective  $H\gamma\gamma$  vertex. In this case, the effect of  $ZH\gamma$  anomaly is also enhanced (15) and the corresponding ultimate value of  $\Lambda_Z$  will be larger.

Figs. 7 and 8 show cross sections of correspondent reactions for different  $\tilde{\Lambda}_i$ . Note that, in contrast to the  $\mathcal{MSM}$  case, the observable effect in  $e\gamma \rightarrow eH$  process increases with growth of energy. This is due to the fact that the  $\mathcal{MSM}$  components of effective couplings  $G_i$  decreases with  $Q^2$  growth in the  $\mathcal{SM}$ , but their anomalous components are  $Q^2$  independent.

We estimated typical values  $\Lambda_i$  which can be observed in the reactions (1) – (3) at the luminosity integral about  $100 \text{ fb}^{-1}$  for the wide interval of possible Higgs boson masses.

For  $\gamma\gamma \rightarrow H$  process we used the following procedure. First, we took into account the branching ratio for the appropriate Higgs boson decay. After that, we estimated the number of main background events (for example,  $\gamma\gamma \rightarrow b\bar{b}$  for  $M_H < 140$  GeV,  $\gamma\gamma \rightarrow ZZ$  for  $M_H > 190$  GeV). Suppose then that the expected number of observed events calculated within  $\mathcal{SM}$  (with the above procedure) be  $N_0$ , while the number of events with considered effect is  $N_0 \pm \Delta N$ . We assume an effect to be observable if either  $\Delta N > 3\sqrt{N_0}$  (provided  $N_0 > 10$ ) or  $\Delta N > 10$  (provided  $N_0 < 10$ ).

For  $e\gamma \rightarrow eH$  process we just compared the  $\mathcal{SM}$  cross section with that calculated in presence of  $Z\gamma H$  anomaly.

The results for both  $\Lambda$  are given in Table 3. Results of a similar analysis of ref. [4] correspond to  $\Lambda_\gamma \sim 10 \div 15$  TeV.

These numbers are only preliminary estimates. To improve the exactitude of these prediction, one should take into account several points. The most important are to perform a thorough background analysis, and to consider the real detector efficiency, which is a subject for specific simulation in each case. Obviously, these effects reduce the ultimate values of  $\Lambda_i$  presented in our Table 3. The  $\mathcal{SM}$  calculations including background for different Higgs boson decays have been done in [13], [15] for the process (1) and in [5] for the process (3). The scale of discussed reduction for  $e\gamma \rightarrow eH$  reaction can be seen from comparison of our results with those obtained in ref. [6] for  $M_H < 140$  GeV. Taking the cross sections obtained there and using our procedure, we found  $\Lambda_Z = 8$  TeV, which should be compared to our estimate  $\Lambda_Z = 11$  TeV for a light Higgs boson.

This comparison shows that our estimates give the correct order of the observability limits. We hope that the same will be true for the other values of Higgs boson mass and consequently other decay modes.

Similar estimates for gluon fusion were obtained in ref. [2]. The results obtained mean in our notation that in future experiments at LHC one can hope to set limitations (for  $\mathcal{CP}$  even anomalous  $ggH$  interactions)  $\Lambda_g = 35$  TeV.

In recent paper [26] some results were reported on  $\gamma\gamma H$  anomaly in  $H\gamma\gamma \rightarrow 3\gamma$  events at Tevatron. The limitations obtained there are weak enough ( $\Lambda_\gamma \approx 1$  TeV) in comparison with numbers from Table 3.

## 4 CONCLUSION

We consider major processes for the Higgs boson production at photon colliders and assess the feasibility of the possible anomalous interactions study. We show that these colliders provide the spectacular field for the investigation of these phenomena. The future experiments at photon and hadron colliders can either reveal or completely rule out new heavy particles that can exist in  $\mathcal{SM}$  before a direct discovery of these heavy particles.

We derive constraints on a characteristic scale of the possible underlying theory that can be obtained from future experiments at  $\gamma\gamma$  or  $\gamma e$  colliders. The analysis of these scales in the framework of some specific models is the subject of further studies. The resultant values of  $\Lambda_i$  are rather large, which makes us believe that the study of the Higgs boson physics at photon colliders will be an important step in probing Nature beyond the Standard Model.

In this paper we analyzed processes which are most appropriate for study of separate anomalies in the effective Lagrangian. From this point of view the investigation of other processes should both support the results obtained from the discussed experiments and give information about new additional anomalies. For instance, the main potential of process  $\gamma\gamma \rightarrow HH$  concerns the study of anomalous Higgs boson self-interaction [27], the main potential of process  $\gamma e \rightarrow \nu WH$  is related to more complex anomalies like  $WWH\gamma$  etc. The study of processes in  $\gamma\gamma$  or  $\gamma e$  collisions have very high potential in these problems since small correction in anomaly is added here not to the relatively large tree effect but to small 1-loop contribution of  $\mathcal{SM}$ .

## Acknowledgements

We are thankful to G. Belanger, F. Boudjema, V.A. Ilyin, A.M. Ryskin, V.G. Serbo for discussions. This work is supported by grants of INTAS – 93 – 1180ext and RFBR 96-02-19079.

## References

- [1] I.F. Ginzburg, I.P. Ivanov, A. Schiller, hep-ph/9802354.
- [2] G.J. Gounaris, J. Layssac and F.M. Renard, hep-ph/9803422.

- [3] I.F. Ginzburg, Preprint 28(182) Inst. of Mathem., Novosibirsk (1990). Main results were reported in *I.F. Ginzburg*, Proc. 9th International Workshop on Photon – Photon Collisions, San Diego (1992) 474–501, World Sc. Singapore.
- [4] G.J. Gounaris, J. Layssac, F.M. Renard. *Z. Phys.* **C65** (1995) 245; G.J. Gounaris, F.M. Renard. hep-ph/9505249; PM/95-20.
- [5] E. Gabrielli, V.A. Ilyin, B Mele, Preprint ROME1-1165/97, NDU-HEP-97-EG01 (1997), hep-ph/9702414, *Phys. Rev.* **D56** (1997) 5945.
- [6] E. Gabrielli, V.A. Ilyin and B. Mele, Proc. "Beyond the Standard Model V", (1997) 506.
- [7] A. Abbasabadi, D. Bowser-Chao, D.A. Dicus and W.A. Repko, *Phys. Rev.* **D52** (1995) 3919.
- [8] P. Bock et al., CERN preprint, Report No. CERN-EP-98-046, 1998; V.Ruhlmann-Kleider, *Search for Higgs bosons at LEP200*, XXXIst Recontres de Moriond, Les Arcs, France, 21–28 March 1998.
- [9] A.I Vainshtein, M.B. Voloshin, V.I. Zakharov, and M.A. Shifman, *Sov. J. Nucl. Phys.* **30** (1979) 711; L.B.Okun, *Leptons and Quarks*. North-Holland Physics Publishing, 1982, Amsterdam.
- [10] I.F.Ginzburg, G.L.Kotkin, V.G.Serbo, V.I.Telnov. *Pis'ma ZhETF* **34** (1981) 514. *Nucl.Instr.Methods (NIM)* **205** (1983) 47. I.F.Ginzburg, G.L.Kotkin, S.L.Panfil, V.G.Serbo, V.I.Telnov. *NIM* **219** (1984) 5.
- [11] Zeroth-order Design Report for the NLC, SLAC Report 474 (1996); TESLA, SBLC Conceptual Design Report, DESY 97-048, ECFA-97-182 (1997); R.Brinkmann et. al., *NIMR* **A406** (1998) 13.
- [12] G.L. Kotkin, V.G. Serbo, *Phys. Lett.* **B413** (1997) 122.
- [13] D.L. Borden, D.A. Bauer, D.O. Caldwell, *Phys. Rev.* **D48** (1993) 4018; D.L. Borden, V.A. Khoze, W.J. Stirling, J.Ohnmus, *Phys. Rev.* **D50** (1994) 4499.
- [14] I.F. Ginzburg, I.P. Ivanov, *Phys. Lett.* **408B** (1997) 325.
- [15] E. Boos et al, DESY 98-004, hep-ph/9801359.
- [16] J.F. Gunion, L. Poggiolli and R. van Kooten, hep-ph/9703330 (1997).
- [17] G.V. Jikia, *Nucl. Phys* **B412** (1994) 57; G.V. Jikia, Yu.F. Pirogov, *Phys. Lett.* **B283** (1992) 135.
- [18] N.N. Achasov, *Phys. Lett.* **B222** (1989) 139.
- [19] O.J.P. Eboli and M.C. Gonzales-Garcia, *Phys. Rev.* **D49** (1994) 91.
- [20] U. Cotti, L.J. Diaz–Cruz and J.J. Toscano, *Phys. Lett.* **B404** (1997) 308
- [21] I.F. Ginzburg, V.G. Serbo, *Phys. Lett.* **103B** (1981) 68.

- [22] G.F. van Oldenborgh, *FF - a package to evaluate one-loop Feynman diagrams*, NIKHE, H/90-15, September 1990; G.F. van Oldenborgh and J.A.M Vermaseren, Z. Phys. **C46** (1990) 425.
- [23] W.Buchmuller, D.Wyler. Nucl.Phys. **B264** (1986) 621.
- [24] C.I.C.Burges, H.I.Schnitzer. Nucl.Phys. **B228** (1983) 464; C.N.Leung, S.T.Love, S.Rao. Z.Phys. **C31** (1986) 433.
- [25] K. Hagiwara et al, Phys. Rev. **D 48** (1993) 2182.
- [26] F. de Campos et al, *hep-ph/9806307*.
- [27] G. Jikia and A. Tkabladze, in: Proc. *Workshop "e<sup>+</sup>e<sup>-</sup> collisions at 500 GeV: the physics potential"*, ed. P.W. Zerwas, DESY 93-123C (1993) p.529; V.A.Ilyin, A.E.Pukhov, Y.Kurihara, Y.Shimizu, T.Kaneko. Phys. Rev. **D 54** (1996) 6717.



# Appendix: Box items

In this appendix we use dilogarithm function  $Li_2(z)$  defined by

$$Li_2(z + i\varepsilon) = - \int_0^z \frac{dt}{t} \ln|1-t| + i\pi\theta(z-1) \ln z.$$

Besides we denote  $t = -Q^2$ ,  $u = M_H^2 - s - t$  and define ( $r_p$  are given by (8))

$$\beta_{P\pm} = \frac{1}{2} \left( 1 \pm \sqrt{1 - r_p} \right), \quad (P = Z, W).$$

The  $Z$  box or  $W$  box item below contains box diagrams and relevant  $s$  and  $u$ -channel triangle diagrams with  $Z$  or  $W$  boson circulating in loops.

## A Z Box items

In the numbering scheme of [7]  $Z$  box item is expressed in terms of scalar loop integrals

$$\begin{aligned} Z(s, u) = & -\frac{(v_e - \zeta_e)^2}{4c_W^4} \frac{1}{2ts} \frac{s - M_Z^2}{s} \left\{ [M_Z^2(s+u) - su] D_Z(1, 2, 3, 4) + s C_Z(1, 2, 3) \right. \\ & + \left( t - s - 2M_Z^2 \frac{ts}{(t+s)(s-M_Z^2)} \right) C_Z(1, 2, 4) - (t+u) C_Z(1, 3, 4) \\ & \left. + u C_Z(2, 3, 4) + \frac{2ts}{(t+s)(s-M_Z^2)} [B_Z(1, 4) - B_Z(2, 4)] \right\}. \end{aligned} \quad (29)$$

Here  $v_e = 1 - 4s_W^2$ . These functions can be evaluated numerically by means of FF package [22]. The full sets of arguments for these functions are:

$$\begin{aligned} D_Z(1, 2, 3, 4) &= D_0(M_Z^2, m_e^2, m_e^2, M_Z^2, 0, 0, 0, M_H^2, s, u); \\ C_Z(1, 2, 3) &= C_0(m_e^2, m_e^2, M_Z^2, 0, 0, s); \\ C_Z(1, 2, 4) &= C_0(m_e^2, M_Z^2, M_Z^2, 0, M_H^2, u); \\ C_Z(1, 3, 4) &= C_0(m_e^2, M_Z^2, M_Z^2, 0, M_H^2, s); \\ C_Z(2, 3, 4) &= C_0(m_e^2, m_e^2, M_Z^2, 0, 0, u); \\ B_Z(1, 4) - B_Z(2, 4) &= B_0(M_Z^2, M_Z^2, M_H^2) - B_0(m_e^2, M_Z^2, u); \end{aligned}$$

Alternatively, we calculated these functions using explicit expressions from [7], rewritten for our process. These formulas have form:

$$\begin{aligned} D_Z(1, 2, 3, 4) = & \frac{1}{su - M_Z^2 s - M_Z^2 u} \left( \left\{ \ln\left(1 - \frac{s}{M_Z^2} - i\varepsilon\right) \left[ \ln\left(\frac{su}{m_e^2 M_H^2} - i\varepsilon\right) + 2 \ln\left(1 - \frac{M_Z^2}{s}\right) \right] \right. \right. \\ & \left. \left. + \ln\left(-\frac{M_Z^2}{s} + i\varepsilon\right) + \ln\left(1 - \frac{M_Z^2}{s} - \frac{M_Z^2}{u}\right) - \ln\left(\beta_{Z+} - \frac{M_Z^2}{s}\right) - \ln\left(\beta_{Z-} - \frac{M_Z^2}{s}\right) \right\} \right) \end{aligned}$$

$$\begin{aligned}
& +2Li_2\left(\frac{-\frac{M_Z^2}{s}}{1-\frac{M_Z^2}{s}}\right) + Li_2\left(\frac{-\frac{M_Z^2}{s}}{1-\frac{M_Z^2}{s}-\frac{M_Z^2}{u}}\right) - Li_2\left(\frac{-\frac{M_Z^2}{s}}{\beta_{Z+}-\frac{M_Z^2}{s}}\right) - Li_2\left(\frac{-\frac{M_Z^2}{s}}{\beta_{Z-}-\frac{M_Z^2}{s}}\right) \\
& - Li_2\left(\frac{1-\frac{M_Z^2}{s}}{1-\frac{M_Z^2}{s}-\frac{M_Z^2}{u}}\right) + Li_2\left(\frac{1-\frac{M_Z^2}{s}}{\beta_{Z+}-\frac{M_Z^2}{s}} - i\varepsilon\right) + Li_2\left(\frac{1-\frac{M_Z^2}{s}}{\beta_{Z-}-\frac{M_Z^2}{s}} + i\varepsilon\right) - \frac{\pi^2}{3} \Big\} \\
& + \left\{ \ln\left(1-\frac{u}{M_Z^2}\right) \left[ \ln\left(\frac{su}{m_e^2 M_H^2} - i\varepsilon\right) + 2\ln\left(1-\frac{M_Z^2}{u}\right) \right. \right. \\
& \left. \left. + \ln\left(-\frac{M_Z^2}{u}\right) + \ln\left(1-\frac{M_Z^2}{u}-\frac{M_Z^2}{s}\right) - \ln\left(\beta_{Z+}-\frac{M_Z^2}{u}\right) - \ln\left(\beta_{Z-}-\frac{M_Z^2}{u}\right) \right] \right\} \\
& +2Li_2\left(\frac{-\frac{M_Z^2}{u}}{1-\frac{M_Z^2}{u}}\right) + Li_2\left(\frac{-\frac{M_Z^2}{u}}{1-\frac{M_Z^2}{u}-\frac{M_Z^2}{s}}\right) - Li_2\left(\frac{-\frac{M_Z^2}{u}}{\beta_{Z+}-\frac{M_Z^2}{u}}\right) - Li_2\left(\frac{-\frac{M_Z^2}{u}}{\beta_{Z-}-\frac{M_Z^2}{u}}\right) \\
& - Li_2\left(\frac{1-\frac{M_Z^2}{u}}{1-\frac{M_Z^2}{u}-\frac{M_Z^2}{s}} - i\varepsilon\right) + Li_2\left(\frac{1-\frac{M_Z^2}{u}}{\beta_{Z+}-\frac{M_Z^2}{u}} - i\varepsilon\right) + Li_2\left(\frac{1-\frac{M_Z^2}{u}}{\beta_{Z-}-\frac{M_Z^2}{u}} + i\varepsilon\right) - \frac{\pi^2}{3} \Big\}.
\end{aligned}$$

$$\begin{aligned}
C_Z(1,2,3) &= \frac{1}{s} \left[ -Li_2\left(\frac{1}{1-\frac{M_Z^2}{s}} - i\varepsilon\right) + \frac{1}{2} \ln^2\left(1-\frac{s}{M_Z^2} - i\varepsilon\right) \right. \\
& \left. - \ln\left(1-\frac{s}{M_Z^2} - i\varepsilon\right) \ln\left(\frac{m_e^2}{M_Z^2}\right) \right];
\end{aligned}$$

$$\begin{aligned}
C_Z(1,2,4) &= \frac{1}{M_H^2 - u} \left[ Li_2\left(\frac{\alpha_1 - 1}{\alpha_1}\right) + Li_2\left(\frac{\alpha_2}{\alpha_2 - \beta_{Z-}}\right) - Li_2\left(\frac{\alpha_2 - 1}{\alpha_2 - \beta_{Z-}} + i\varepsilon\right) \right. \\
& + Li_2\left(\frac{\alpha_2}{\alpha_2 - \beta_{Z+}}\right) - Li_2\left(\frac{\alpha_2 - 1}{\alpha_2 - \beta_{Z+}} - i\varepsilon\right) - Li_2\left(\frac{\alpha_3}{\alpha_3 - 1}\right) \\
& \left. - Li_2\left(\frac{\alpha_3}{\alpha_3 - \frac{M_Z^2}{u}}\right) + Li_2\left(\frac{\alpha_3 - 1}{\alpha_3 - \frac{M_Z^2}{u}}\right) \right];
\end{aligned}$$

$$\begin{aligned}
C_Z(1, 3, 4) &= \frac{1}{M_H^2 - s} \left[ Li_2 \left( \frac{\gamma - 1}{\gamma - 1 + \frac{M_Z^2}{s}} - i\varepsilon \right) - Li_2 \left( \frac{\gamma}{\gamma - 1 + \frac{M_Z^2}{s}} \right) + Li_2 \left( \frac{\gamma - 1}{\gamma} + i\varepsilon \right) \right. \\
&\quad \left. + Li_2 \left( \frac{\gamma}{\gamma - \beta_{Z-}} \right) - Li_2 \left( \frac{\gamma - 1}{\gamma - \beta_{Z-}} + i\varepsilon \right) + Li_2 \left( \frac{\gamma}{\gamma - \beta_{Z+}} \right) - Li_2 \left( \frac{\gamma - 1}{\gamma - \beta_{Z+}} - i\varepsilon \right) - \frac{\pi^2}{6} \right]; \\
C_Z(2, 3, 4) &= \frac{1}{u} \left[ -Li_2 \left( \frac{1}{1 - \frac{M_Z^2}{u}} \right) + \frac{1}{2} \ln^2 \left( 1 - \frac{u}{M_Z^2} \right) - \ln \left( 1 - \frac{u}{M_Z^2} \right) \ln \left( \frac{m_e^2}{M_Z^2} \right) \right]. \\
B_Z(1, 4) - B_Z(2, 4) &= \sqrt{1 - r_Z} \ln \left( \frac{-\beta_{Z-}}{\beta_{Z+}} + i\varepsilon \right) - \left( 1 - \frac{M_Z^2}{u} \right) \ln \left( \frac{M_Z^2}{M_Z^2 - u} \right).
\end{aligned}$$

Here

$$\begin{aligned}
\alpha_1 &= \frac{u^2 - M_H^2 u + M_H^2 M_Z^2}{(M_H^2 - u)^2}, & \alpha_2 &= \frac{M_Z^2}{M_H^2 - u}, \\
\alpha_3 &= \frac{M_Z^2 M_H^2}{u(M_H^2 - u)}, & \gamma &= \frac{M_Z^2}{M_H^2 - s}.
\end{aligned}$$

When  $u$  and  $s$  are switched in the above formulas,  $D_0$  does not change at all, while  $C_Z(1, 2, 3) \leftrightarrow C_Z(2, 3, 4)$ ,  $C_Z(1, 2, 4) \leftrightarrow C_Z(1, 3, 4)$ . Note also that terms containing  $\ln(m_e^2)$  finally cancel each other in (29).

## B W box items

The W box item can be written as a sum of two functions:

$$W(s, u) = (1 - \zeta_e) (A_1(t, s, u) + A_2(t, u, s)) \quad (30)$$

with the following decomposition:

$$\begin{aligned}
A_1(t, s, u) &= \frac{1}{2ts} \frac{s - M_W^2}{s} \left\{ (ts + M_W^2 (s + u)) D_W(1, 2, 3, 4) + \left[ -tC_W(1, 2, 3) \right. \right. \\
&\quad \left. \left. + (t + u)C_W(1, 2, 4) - (s + u)C_W(1, 3, 4) + sC_W(2, 3, 4) \right] \right. \\
&\quad \left. - \frac{2ts}{(s + u)(s - M_W^2)} [B_W(1, 3) - B_W(1, 4)] \right\}. \quad (31)
\end{aligned}$$

$$\begin{aligned}
A_2(t, s, u) &= \frac{1}{2tu} \frac{t + u - M_W^2}{u} \left\{ \left[ (M_W^2 (s + u) - ts) - 2M_W^2 t \right] D_W(1, 2, 3, 4) \right. \\
&\quad \left. + \left[ tC_W(1, 2, 3) + \frac{u^2 - 2tu - t^2}{t + u} C_W(1, 2, 4) - (s + u)C_W(1, 3, 4) \right] \right\}
\end{aligned}$$

$$\begin{aligned}
& +sC_W(2, 3, 4) \Big] + \frac{2tu}{(s+u)(t+u-M_W^2)} [B_W(1, 3) - B_W(1, 4)] \\
& + \frac{2tu}{(t+u)(t+u-M_W^2)} [B_W(2, 4) - B_W(1, 4)] \Big\}; \quad (32)
\end{aligned}$$

Again, full arguments for evaluating these scalar loop integrals with FF are:

$$\begin{aligned}
D_W(1, 2, 3, 4) &= D_0(M_W^2, 0, M_W^2, M_W^2, 0, 0, 0, M_H^2, t, s); \\
C_W(1, 2, 3) &= C_0(0, M_W^2, M_W^2, 0, t, 0); \\
C_W(1, 2, 4) &= C_0(0, M_W^2, M_W^2, 0, M_H^2, s); \\
C_W(1, 3, 4) &= C_0(M_W^2, M_W^2, M_W^2, t, 0, M_H^2); \\
C_W(2, 3, 4) &= C_0(0, M_W^2, M_W^2, 0, 0, s); \\
B_W(1, 3) - B_W(1, 4) &= B_0(M_W^2, M_W^2, t) - B_0(M_W^2, M_W^2, M_H^2); \\
B_W(2, 4) - B_W(1, 3) &= B_0(0, M_W^2, s) - B_0(M_W^2, M_W^2, M_H^2);
\end{aligned}$$

We used decomposition of these functions in dilogarithms etc. with using auxiliary notations

$$\begin{aligned}
\alpha &= 1 - \frac{M_W^2}{s}, \quad \gamma_{\pm} = \frac{1}{2} \left( 1 \pm \sqrt{1 - \frac{r_W}{w}} \right), \\
\lambda_{\pm} &= \frac{1}{2} \left[ 1 + \frac{M_W^2(t - M_H^2)}{-ts} \pm \sqrt{\left( 1 + \frac{M_W^2(t - M_H^2)}{-ts} \right)^2 - \frac{4M_W^2}{t}} \right]. \quad (33)
\end{aligned}$$

$$\begin{aligned}
D_W(1, 2, 3, 4) &= -\frac{1}{ts(\lambda_+ - \lambda_-)} \left\{ \left[ -Li_2 \left( \frac{1 - \lambda_+}{\alpha - \lambda_+} \right) + Li_2 \left( \frac{-\lambda_+}{\alpha - \lambda_+} + i\varepsilon \right) \right. \right. \\
& - Li_2 \left( \frac{1 - \lambda_+}{\gamma_+ - \lambda_+} \right) + Li_2 \left( \frac{-\lambda_+}{\gamma_+ - \lambda_+} \right) - Li_2 \left( \frac{1 - \lambda_+}{\gamma_- - \lambda_+} \right) \\
& + Li_2 \left( \frac{-\lambda_+}{\gamma_- - \lambda_+} \right) + Li_2 \left( \frac{1 - \lambda_+}{\beta_{W_+} - \lambda_+} \right) - Li_2 \left( \frac{-\lambda_+}{\beta_{W_+} - \lambda_+} + i\varepsilon \right) \\
& \left. + Li_2 \left( \frac{1 - \lambda_+}{\beta_{W_-} - \lambda_+} \right) - Li_2 \left( \frac{-\lambda_+}{\beta_{W_-} - \lambda_+} - i\varepsilon \right) \right] \\
& - \left[ -Li_2 \left( \frac{1 - \lambda_-}{\alpha - \lambda_-} - i\varepsilon \right) + Li_2 \left( \frac{-\lambda_-}{\alpha - \lambda_-} \right) - Li_2 \left( \frac{1 - \lambda_-}{\gamma_+ - \lambda_-} \right) + Li_2 \left( \frac{-\lambda_-}{\gamma_+ - \lambda_-} \right) \right. \\
& - Li_2 \left( \frac{1 - \lambda_-}{\gamma_- - \lambda_-} + i\varepsilon \right) + Li_2 \left( \frac{-\lambda_-}{\gamma_- - \lambda_-} + i\varepsilon \right) + Li_2 \left( \frac{1 - \lambda_-}{\beta_{W_+} - \lambda_-} - i\varepsilon \right) \\
& \left. - Li_2 \left( \frac{-\lambda_-}{\beta_{W_+} - \lambda_-} \right) + Li_2 \left( \frac{1 - \lambda_-}{\beta_{W_-} - \lambda_-} + i\varepsilon \right) - Li_2 \left( \frac{-\lambda_-}{\beta_{W_-} - \lambda_-} \right) \right] \Big\} \\
C_W(1, 2, 3) &= \frac{1}{t} \left[ -\frac{\pi^2}{6} + Li_2 \left( 1 - \frac{t}{M_W^2} + i\varepsilon \right) + Li_2 \left( \frac{M_W^2}{M_W^2 - t\gamma_+} \right) \right]
\end{aligned}$$

$$-Li_2\left(\frac{M_W^2 - t}{M_W^2 - t\gamma_+}\right) + Li_2\left(\frac{M_W^2}{M_W^2 - t\gamma_-} + i\varepsilon\right) - Li_2\left(\frac{M_W^2 - t}{M_W^2 - t\gamma_-} + i\varepsilon\right),$$

$$C_W(1, 3, 4) = \frac{1}{M_H^2 - t} \left[ Li_2\left(\frac{1}{\gamma_+}\right) + Li_2\left(\frac{1}{\gamma_-}\right) - Li_2\left(\frac{1}{\beta_{W+}} - i\varepsilon\right) - Li_2\left(\frac{1}{\beta_{W-}} + i\varepsilon\right) \right]$$

$$C_W(2, 3, 4) = -\frac{1}{s} Li_2\left(\frac{s}{M_W^2} + i\varepsilon\right),$$

and  $C_W(1, 2, 4)$  can be obtained from  $C_Z(1, 3, 4)$  by replacing  $m_Z \rightarrow m_W$ .

$$B_W(1, 3) - B_W(1, 4) = \sqrt{1 + \frac{r_W}{w}} \ln\left(-\frac{\gamma_-}{\gamma_+}\right) - \sqrt{1 - r_W} \ln\left(-\frac{\beta_{W-}}{\beta_{W+}} + i\varepsilon\right)$$

$$B_W(2, 4) - B_W(1, 4) = \left(1 - \frac{M_W^2}{s}\right) \ln\left(\frac{M_W^2}{M_W^2 - s} + i\varepsilon\right) - \sqrt{1 - r_W} \ln\left(-\frac{\beta_{W-}}{\beta_{W+}} + i\varepsilon\right).$$

$\sqrt{s} = 1.5 \text{ TeV} \quad Q^2 = 1000 \text{ GeV}^2$					
$M_H = 100 \text{ GeV}$					
$\zeta_e, \lambda_\gamma$	$ \gamma\gamma H ^2, fb$	$\gamma Z\text{-int.}, fb$	$ \gamma ZH ^2, fb$	pole-box int., $fb$	$ box ^2, fb$
-1; -1	0.929	0.852	0.273	-0.0160	0.0105
-1; +1	0.903	0.811	0.253	0.0363	0.0034
+1; -1	0.903	-0.700	0.188	1.3e-6	1.2e-5
+1; +1	0.929	-0.735	0.203	-2.5e-4	2.5e-4
$\sigma_L = 2.03 fb, \quad \sigma_R = 0.39 fb, \quad \sigma^{np} = 1.21 fb, \quad \Delta\sigma = 1.64 fb$					
$M_H = 200 \text{ GeV}$					
$\zeta_e, \lambda_\gamma$	$ \gamma\gamma H ^2, fb$	$\gamma Z\text{-int.}, fb$	$ \gamma ZH ^2, fb$	pole-box int., $fb$	$ box ^2, fb$
-1; -1	2.06	1.77	0.537	0.0200	0.0234
-1; +1	1.96	1.65	0.490	0.0702	0.0038
+1; -1	1.96	-1.43	0.364	-7.0e-5	1.4e-5
+1; +1	2.06	-1.53	0.399	-5.2e-4	5.0e-4
$\sigma_L = 4.29 fb, \quad \sigma_R = 0.91 fb, \quad \sigma^{np} = 2.60 fb, \quad \Delta\sigma = 3.38 fb$					
$M_H = 500 \text{ GeV}$					
$\zeta_e, \lambda_\gamma$	$ \gamma\gamma H ^2, fb$	$\gamma Z\text{-int.}, fb$	$ \gamma ZH ^2, fb$	pole-box int., $fb$	$ box ^2, fb$
-1; -1	0.059	0.083	0.085	0.0056	0.0144
-1; +1	0.045	0.066	0.061	0.0163	0.0032
+1; -1	0.045	-0.057	0.045	-5.9e-5	4.8e-6
+1; +1	0.059	-0.072	0.063	-0.0013	1.5e-4
$\sigma_L = 0.22 fb, \quad \sigma_R = 0.05 fb, \quad \sigma^{np} = 0.13 fb, \quad \Delta\sigma = 0.17 fb$					

Table 1: The cross section of  $e\gamma \rightarrow eH$  for various polarization states.

$\sqrt{s} = 1.5 \text{ TeV}$						
$Q^2,$ $\text{GeV}^2$	$M_H = 100 \text{ GeV}$		$M_H = 200 \text{ GeV}$		$M_H = 500 \text{ GeV}$	
	$\sigma_{np}, fb$	$\Delta\sigma, fb$	$\sigma_{np}, fb$	$\Delta\sigma, fb$	$\sigma_{np}, fb$	$\Delta\sigma, fb$
1	3.23	1.75	7.42	3.65	0.26	0.19
3	2.90	1.75	6.65	3.65	0.24	0.19
10	2.56	1.75	5.81	3.65	0.21	0.19
30	2.23	1.75	5.04	3.64	0.19	0.19
100	1.88	1.74	4.20	3.62	0.17	0.19
300	1.56	1.71	3.44	3.57	0.15	0.19
1000	1.21	1.63	2.61	3.38	0.13	0.18
3000	0.89	1.44	1.86	2.94	0.11	0.16
10000	0.55	1.02	1.08	1.98	0.08	0.11
30000	0.27	0.53	0.49	0.96	0.05	0.06

Table 2:  $Q^2$  dependence of  $\Delta\sigma$  and  $\sigma_{np}$ .

$M_H, \text{ GeV}$	$\Lambda_\gamma, \text{ TeV}$	$\Lambda_Z, \text{ TeV}$
100	60	11
200	45	9
300	28	8
400	12	7
500	10	8
700	10	10

Table 3: Values of  $\Lambda_i$  for different  $M_H$  which can be probed at photon colliders.

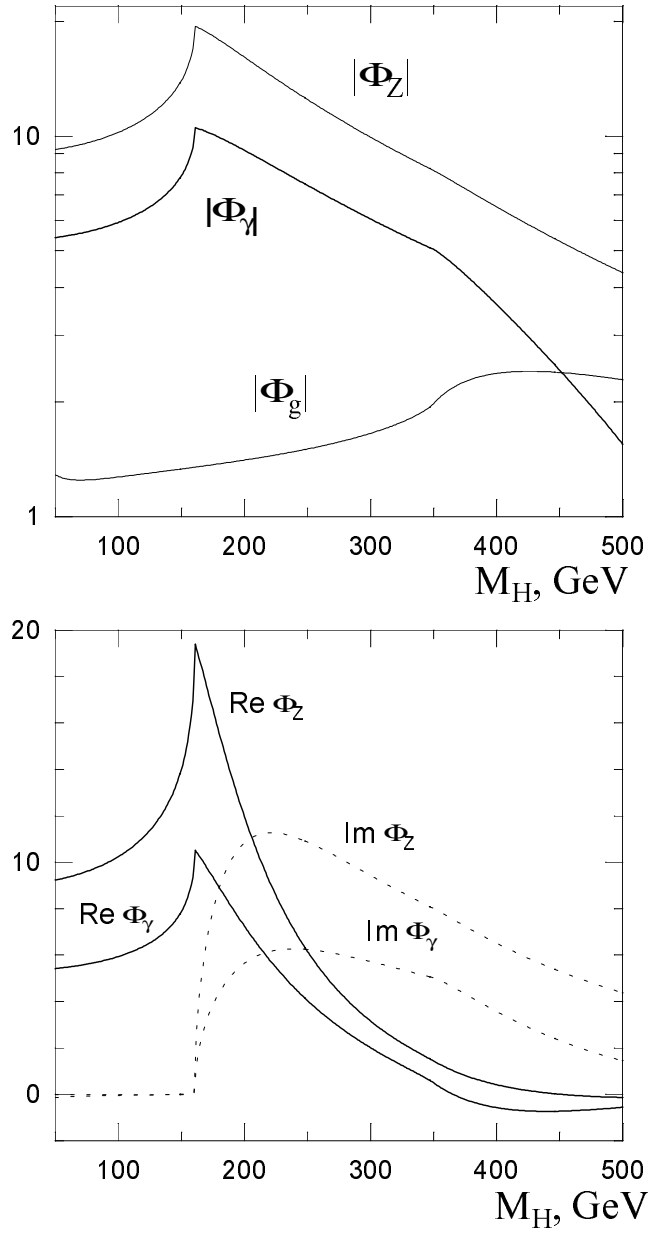


Figure 1: Loop integrals for  $\gamma\gamma H$  and  $Z\gamma H$  interactions: absolute values and real and imaginary parts. The same loops integral for  $ggH$  interaction is also shown for comparison.



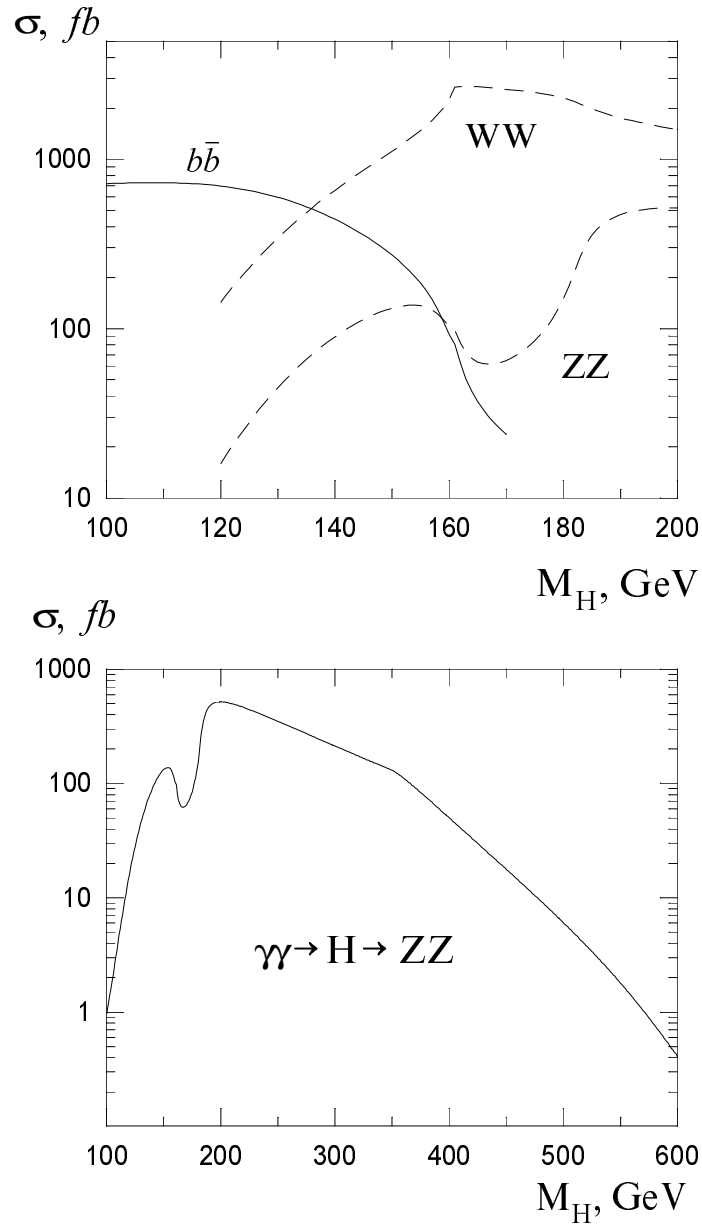


Figure 2: Higgs boson production cross section in reaction  $\gamma\gamma \rightarrow H$  with important Higgs boson decay channels.  $\langle \lambda_1 \rangle = \langle \lambda_2 \rangle = 0.9$ ;  $20^\circ < \theta < 160^\circ$ .

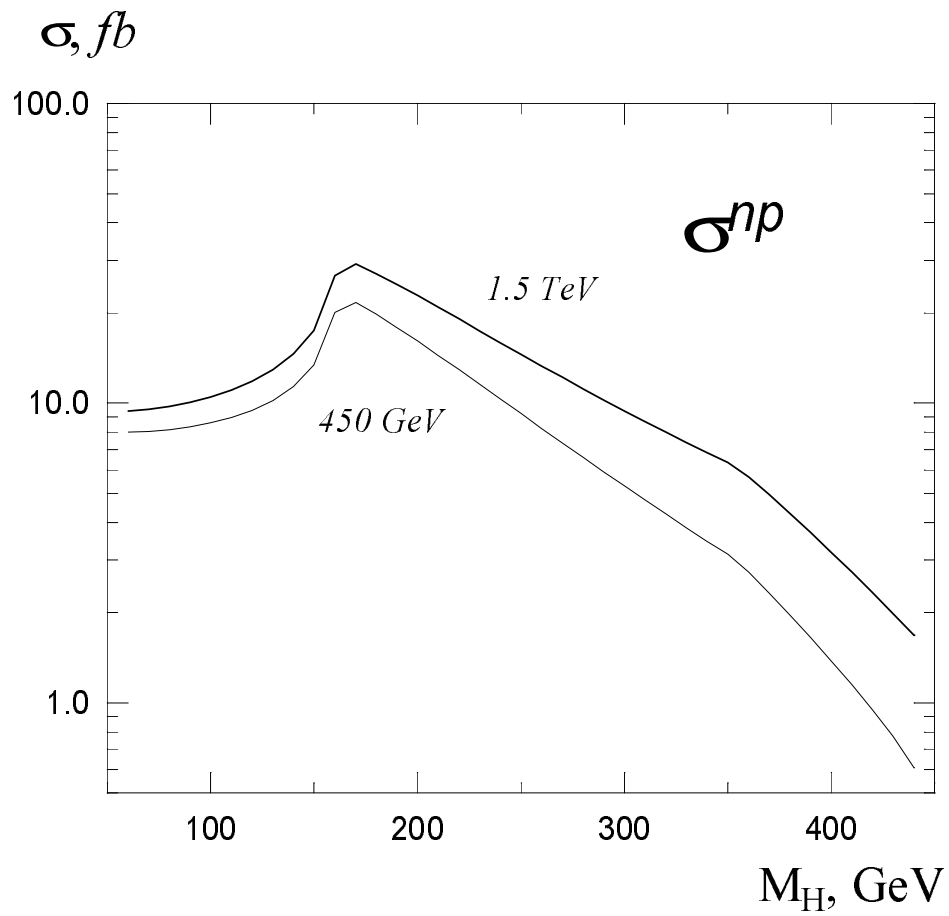


Figure 3: Total unpolarized  $e\gamma \rightarrow eH$  cross section for  $\sqrt{s} = 450$  GeV and 1.5 TeV.

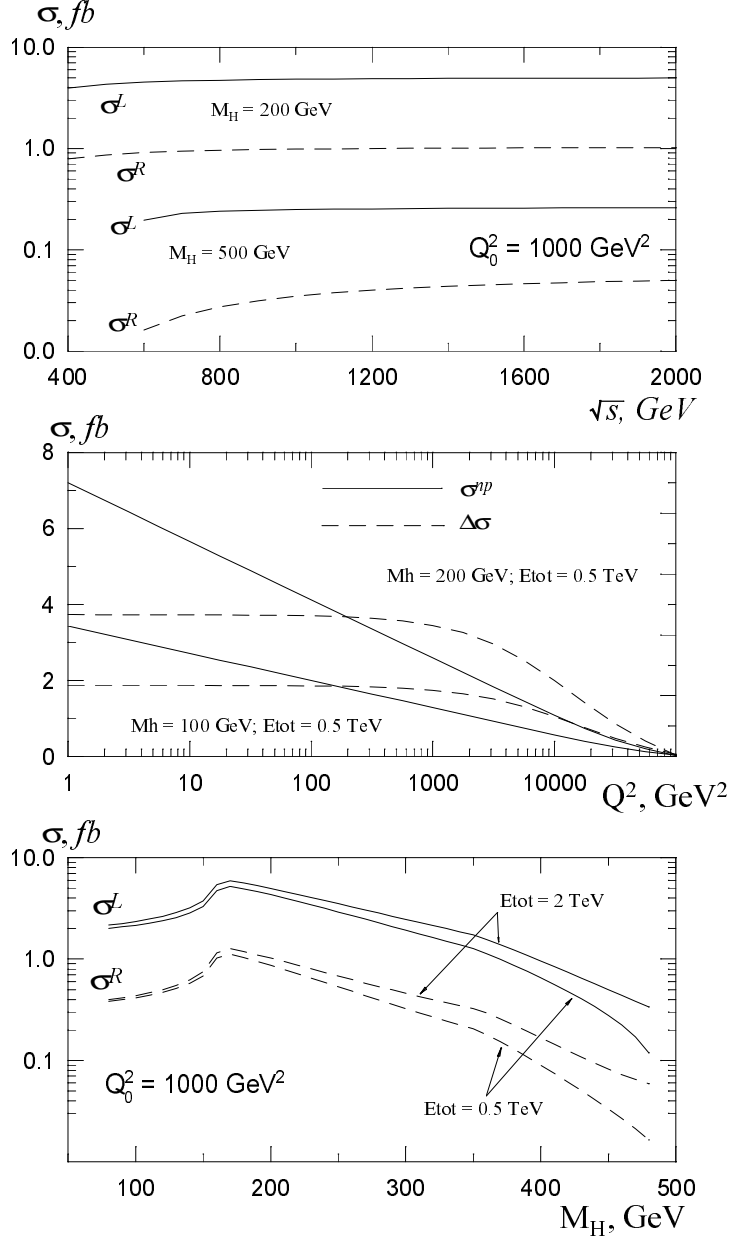


Figure 4: Various dependences of  $e\gamma \rightarrow eH$  cross section:  $s$ -dependence of  $\sigma_L$  and  $\sigma_R$  (upper),  $Q^2$ -dependence of  $\sigma^{np}$  and  $\Delta\sigma$  (middle) and  $M_H$ -dependence for  $\sigma_L$  and  $\sigma_R$  (lower).

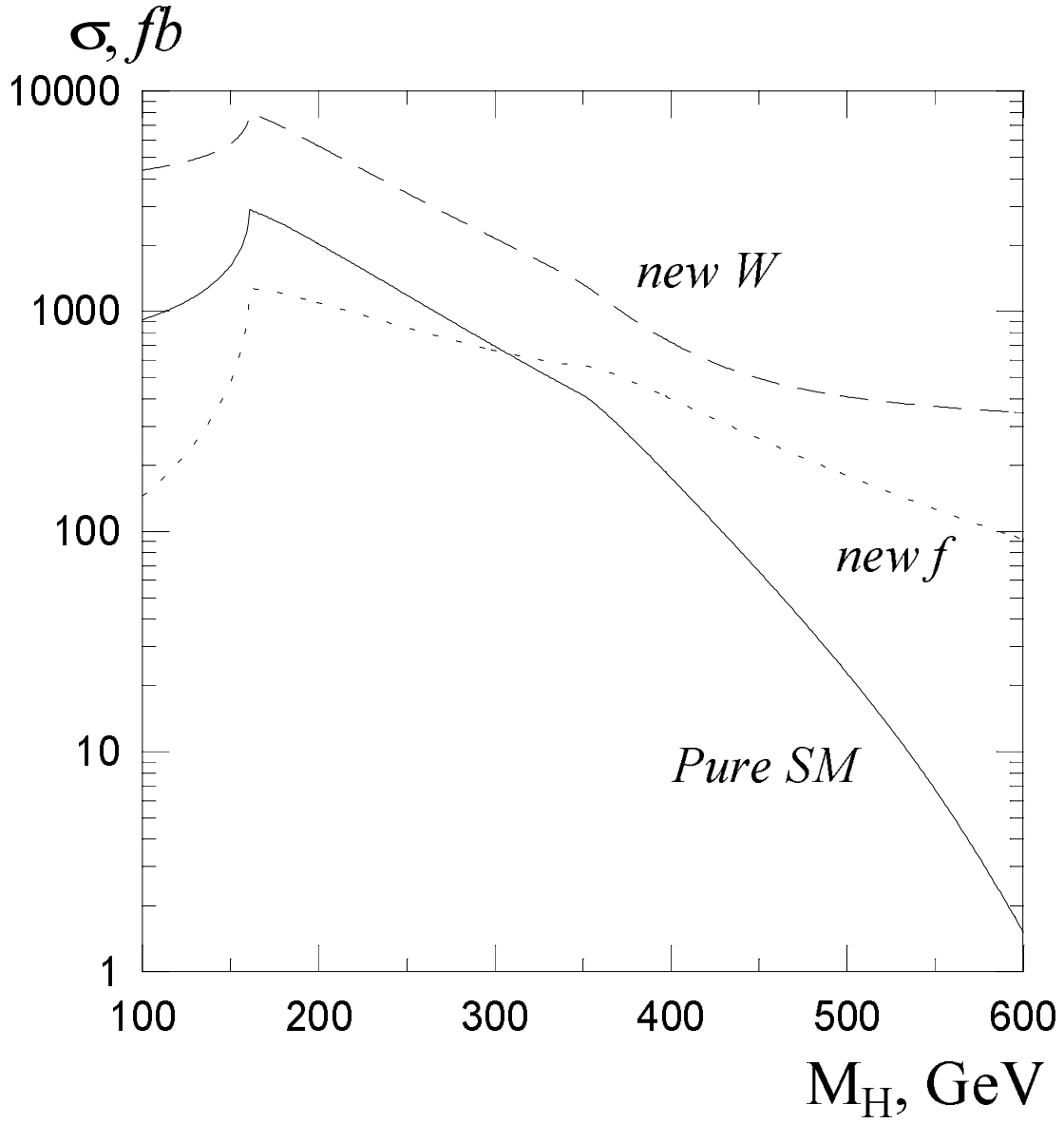


Figure 5: The effect of new particles within  $\mathcal{SM}$  on  $\gamma\gamma \rightarrow H$  cross section.  $\langle \lambda_1 \rangle = \langle \lambda_2 \rangle = 0.9$ ;  $20^\circ < \theta < 160^\circ$ .

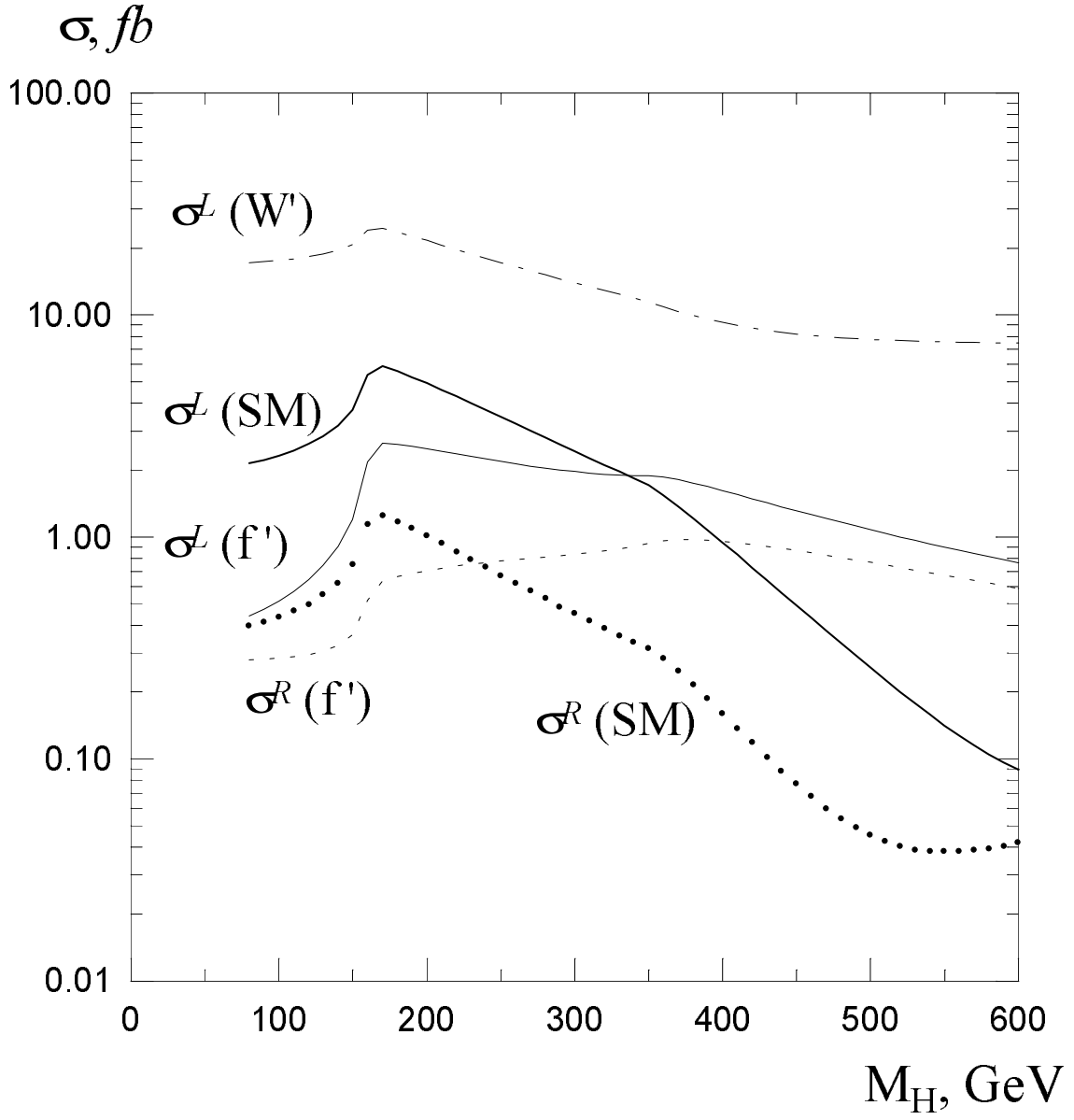


Figure 6: The effect of new particles with  $SM$  on  $e\gamma \rightarrow eH$  cross section.  $\sqrt{s} = 1.5$  TeV,  $Q^2 = 1000$  GeV<sup>2</sup>.

$$\sigma(\gamma\gamma \rightarrow H) / \sigma(\gamma\gamma \rightarrow H)_{SM}$$

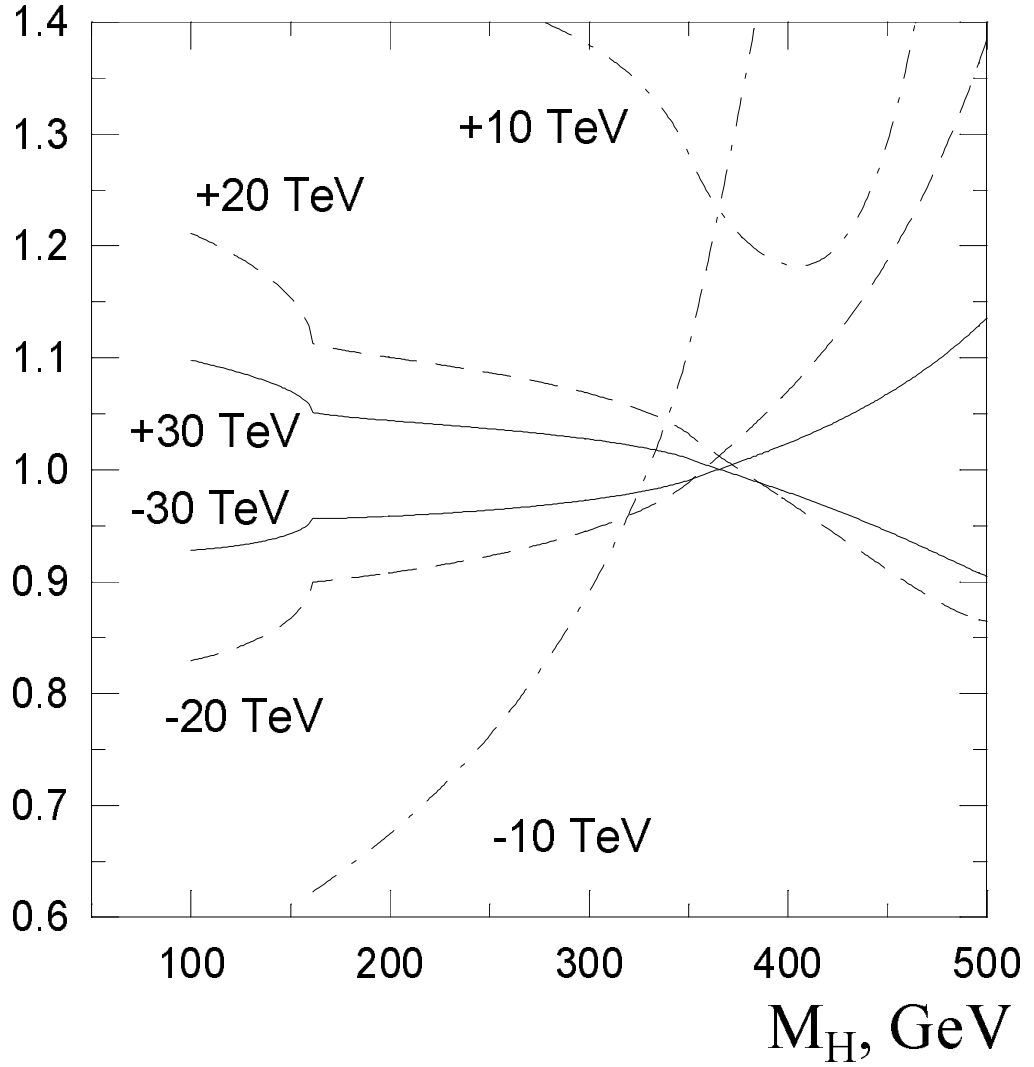


Figure 7: The relative modification of the  $\gamma\gamma \rightarrow H$  cross section compared to its  $SM$  value caused by anomalous interactions. The numbers denote  $\tilde{\Lambda}_\gamma$ .

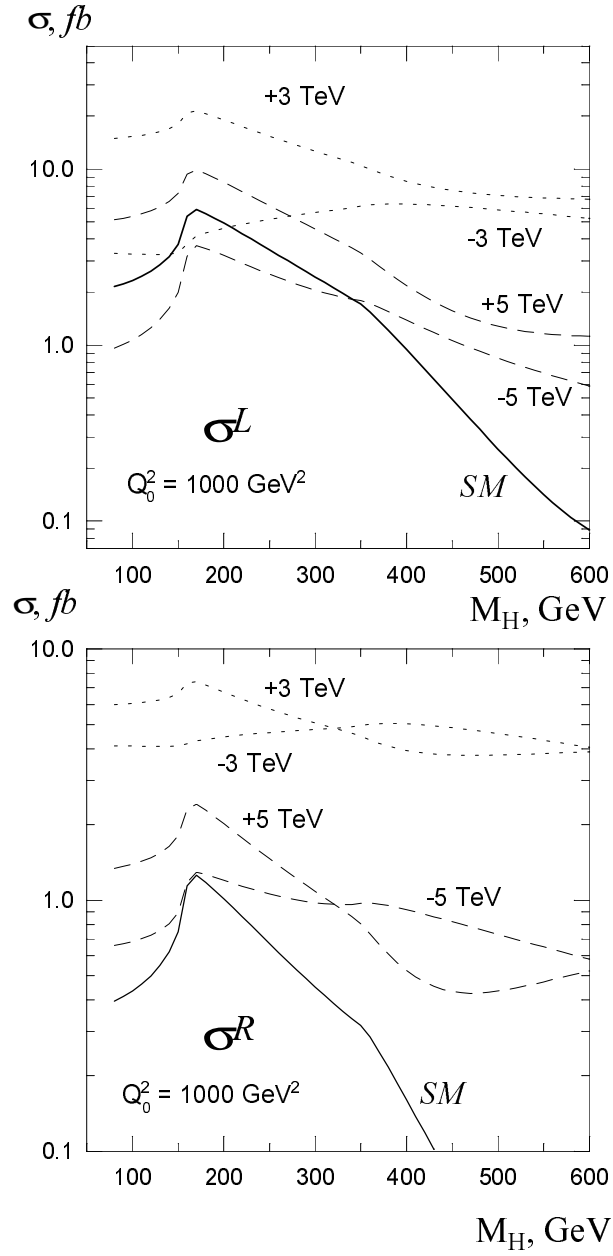


Figure 8: The modification of  $\sigma_L$  and  $\sigma_R$  cross sections of  $e\gamma \rightarrow eH$  caused by  $Z\gamma H$  anomaly. The numbers denote  $\tilde{\Lambda}_Z$ .